Journal of Dental Sciences 19 (2024) 607–613

Available online at www.sciencedirect.com

ScienceDirect

journal homepage: www.e-jds.com

Original Article

Effect of different implant locations and abutment types on stress and strain distribution under non-axial loading: A 3-dimensional finite element analysis

Didem Sakar [a], Mustafa Baris Guncu [a], Hale Arikan [b], Mehmet Muhtarogullari [a], Guliz Aktas [a], Natalia Reiss [c], Ilser Turkyilmaz [d*]

[a] *Department of Prosthodontics, School of Dentistry, Hacettepe University, Ankara, Turkey*
[b] *Department of Prosthodontics, Faculty of Dentistry, Baskent University, Ankara, Turkey*
[c] *New York University College of Dentistry, New York, NY, USA*
[d] *Department of Prosthodontics, New York University College of Dentistry, New York, NY, USA*

Received 22 October 2023; Final revision received 5 November 2023
Available online 11 November 2023

KEYWORDS
Abutment;
Finite element;
Implant;
Strain;
Stress

Abstract *Background/purpose:* Dental implants have been a popular treatment for replacing missing teeth. The purpose of this study was to investigate the impact of engaging (hexagonal) and non-engaging (non-hexagonal) abutments in various six-unit fixed prosthesis on the stress distribution and loading located in the implant neck, implant abutment, and surrounding bone.
Materials and methods: Three implants were digitally designed and inserted parallel to each other in edentulous sites of the maxillary right canine, maxillary right central incisor, and maxillary left canine. Titanium base engaging abutments, non-engaging abutments and connecting screws were designed. Five distinct models of 6-unit fixed dental prosthesis were created, each featuring different combinations of various abutments. Forces (45-degree angle) were applied to the prosthesis, allowing for the analysis of the stress distribution on the implant neck and abutments, and the maximum and minimum principal stress values on the cortical and trabecular bone.
Results: Von Mises stress values and stress distributions located in the implant neck region due to the applied loading forces were analyzed. The overall stress values were highest while employing the hexagonal abutments. The maxillary left canine with a hexagonal abutment (model 5) reported the highest von mises value (64.71 MPa) while the maxillary right canine with a non-hexagonal abutment (model 4) presented lowest von mises value (56.69 MPa).
Conclusion: The results suggest that both the various abutment combinations (engaging and

* Corresponding author. New York University College of Dentistry, Department of Prosthodontics, 380 Second Avenue, Suite 302, New York, NY, 10010, USA.
E-mail address: ilserturkyilmaz@yahoo.com (I. Turkyilmaz).

https://doi.org/10.1016/j.jds.2023.11.001
1991-7902/© 2023 Association for Dental Sciences of the Republic of China. Publishing services by Elsevier B.V. This is an open access article under the CC BY-NC-ND license (http://creativecommons.org/licenses/by-nc-nd/4.0/).

non-engaging) on five different models have a similar influence on the distribution of stress within the implant system.
© 2023 Association for Dental Sciences of the Republic of China. Publishing services by Elsevier B.V. This is an open access article under the CC BY-NC-ND license (http://creativecommons.org/licenses/by-nc-nd/4.0/).

Introduction

While dental implants have been a popular treatment for replacing missing dentition,[1–3] the two differ in biomechanical conditions during functional loading. Natural dentition and implants both have similar soft tissue attachment which maintains a stable seal.[4,5] However, due to the weaker attachment between soft tissue and implants, comparable to that of free gingiva, there is a higher risk of soft tissue collapse under stress. In addition, occlusal forces in natural dentition are typically transferred to the periodontal ligament which contain protective shock-absorbing function while these forces in implants are directly relocated to bone. While an increase in stress in bone can lead to higher bone density, forces exceeding certain threshold may result bone resorption instead of apposition.[6,7] Consequently, implants are unable to adapt to certain restorations and excessive occlusal load, leading to complications in the oral cavity. Critical factors in the success of these implants are the quality and quantity of bone, patient's parafunctional habits, restorative plan, as well as type of implant used.[8–10] Components of such implants include number used to support prosthesis, length, type of connection and abutment, and distribution of a long span prosthesis.[11,12]

Engaging (hexagonal) abutments are able to lock into the shape of the implant, creating anti-rotational mechanism for any restoration that might rotate such as a single unit implant crown.[13,14] These engaging abutments can also be used for multi-unit implant supported fixed prosthesis if the implants are positioned parallel to one another, and the path of insertion is aligned. However, non-engaging (non-hexagonal abutments) lack the anti-rotational component and thus, ease the difficulty of restoring these multi-unit prosthesis by compensating for the mis-angulation and deviation.[15–17] They allow for correction of implant positioning, enabling the creation of a more parallel path for the prosthetic components.[16,17] In addition, hexagonal abutments provide better stability due to an increased height of 5.5 mm compared to non-hexagonal abutment with a standard height of 3.5 mm. Hence, the selection of hexagonal verses non-hexagonal abutments during restorative treatment planning primarily hinges on the position and angulation of the implants placed. Nonetheless, optimizing implant success may involve incorporating a combination of both non-hexagonal and hexagonal abutments, particularly in cases where fixed multi-unit prosthetic restorations are supported by implants. Ultimately, the choice of abutments during dental implant restorative treatment planning should be based on a careful evaluation of the individual patient's anatomical features, implant positioning, esthetic requirements, and functional considerations. The overall objective is to achieve long-term implant success, function, and esthetics while addressing any unique challenges presented by the patient's clinical situation.

The aim of this study was to evaluate how different combinations of hexagonal and non-hexagonal abutments in a six-unit fixed prosthesis affect the distribution of stress and loading on the implant neck, implant abutment, and surrounding bone.

Materials and methods

One experienced clinician designed a partially edentulous maxillary model by using a software (3D Slicer, www.slicer.org) which utilized cone-beam computed-tomography (CBCT) data of a patient. Then, three implants (4.1 mm × 10 mm, Straumann AG, Basel, Switzerland) were digitally designed and inserted parallel to each other in edentulous space of the maxillary right canine, maxillary right central incisor, and maxillary left canine. Titanium base engaging abutments, non-engaging abutments (GH: 1 mm, AH: 3.5 mm, Straumann Variobase) and connecting screws were designed with accordance to the implant catalog data. Additionally, a cement with a thickness of 50 μm was created with reference to the outer surface of the abutment in order to mimic clinical conditions. Appropriate anatomical teeth were digitally designed on the model. The height of the central, lateral, and canine was 10 mm, and a 6-unit fixed dental prosthesis (FDP) fabricated from translucent monolithic zirconia superstructure model was created. Oblique forces (45-degree angle) were applied to the cingulum area of the restorations and thus, Von Mises stress values on the implant neck and abutments, and the maximum and minimum principal stress values on the cortical and trabecular bone were investigated.

A total of 5 different models were generated, each with different combinations utilizing the hexagonal and non-hexagonal abutments (Fig. 1). The following combinations of abutments were created in the position of the maxillary right canine (#13), maxillary right central incisor (#11), and maxillary left canine (#23):

Model 1: Hexagonal, non-hexagonal, non-hexagonal
Model 2: Hexagonal, hexagonal, non-hexagonal
Model 3: Non-hexagonal, hexagonal, non-hexagonal
Model 4: Non-hexagonal, non-hexagonal, non-hexagonal
Model 5: Hexagonal, hexagonal, hexagonal

A maxillary bone model was created using open source data from Visible Human Project (The National Library of

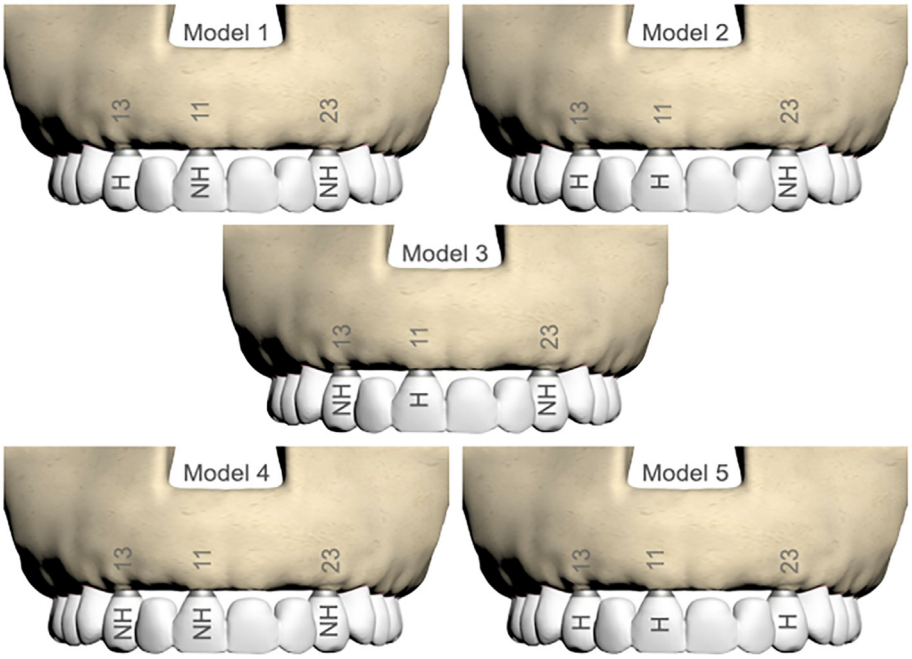

Fig. 1 Five models of various abutment combinations.

Medicine; Fact Sheets Office of Communications and Public Liaison National Library of Medicine, Bethesda, MD, USA). CBCT data in DICOM (Digital Imaging and Communications in Medicine) format was analyzed and divided according to the proper Hounsfield values by using a software (3D Slicer) to analyze the density. Briefly, 3D Slicer is a free, open source software for visualization, processing, segmentation, and analysis of medical, biomedical, and other 3D images and meshes; and planning and navigating image-guided procedures. Afterwards, the data was converted into a three-dimensional (3D) model by segmentation and exported in the standard triangle language (STL) format. The 3D model was transferred to another software (Altair Evolve software, Altair Engineering Inc., Troy, MI, USA), and 1.5 mm thick cortical bone was generated with a 1.5 mm offset to the maxilla cortical bone model, creating a Class 1 occlusion. Trabecular bone was created by using the 3D model of the maxilla cortical bone but adjusting accordingly to the proper bone density. The five models were positioned in the appropriate coordinates of the 3D space in the software (Altair Evolve).

The mathematical models were created by simplifying the geometric models into smaller pieces called meshes by using a software (Altair Hypermesh). Afterwards, these models were converted into. fem format by using a program (Altair Optistruct) to undergo proper analysis. To analyze the created mathematical models and obtain appropriate results, the model's surface relations were defined in the analysis program.

A total force of 300 N was applied at a 45° angle in a palatolabial direction to the cingulum of the right maxillary canine, right maxillary central incisor and left maxillary canine in all five models (Fig. 2). A total of 50 N was applied to each tooth. A linear static analysis was performed for each of the five models under a single loading condition.

A computer program (Altair Optistruct) can provide 25 different stress values obtained by finite element stress analysis. Two groups can be made from the stresses resulting from loading: compression and tensile stresses (symbolized by σ) and shear stresses (symbolized by τ).

The greatest stress value occurs when the components of the total shear stresses equal to zero. In such a situation, normal stresses are called principal stresses. These are divided into three stresses: maximum principal stress, intermediate principal stress, and minimum principal stress. In general, $\sigma 1$ represents maximum principal stress and the largest positive value, $\sigma 3$ indicates the minimum principal stress and the smallest negative value, and $\sigma 2$ is an intermediate value.

When analyzing the results, tensile stresses are represented by the positive values and compression stresses are represented by the negative values. The stress that has the larger absolute value in a stress element is the stress type that influences the stress element, and thus, should be analyzed. The principal stress value is an important factor when evaluating brittle material such as bone. When maximum principal stress is equal to or greater than the maximum tensile strength and the absolute value of the minimum principal stress is equal to or greater than the maximum compressive strength then failure occurs.

The following parameters were used for the finite element analysis in this study. Linear, isotropic material properties used in this study were presented in Table 1.

Boundary conditions:

a) Constraints: All models were fixed from the nodes on the superior region of the cortical and trabecular bone, so that movement was constrained in all three directions.
b) Loading condition: In all models, a total force of 300 N was applied to the cingulum of the central, lateral and

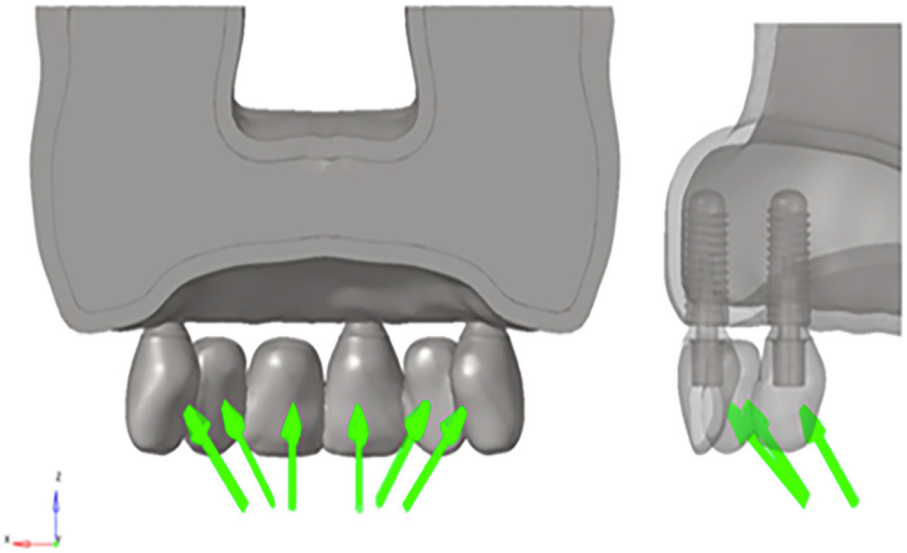

Fig. 2 Forces were applied at a 45° angle in a palatolabial direction to the cingulum of the right maxillary canine, right maxillary central incisor and left maxillary canine in all five models.

Table 1 Linear, isotropic material properties used in this study.

Material	Elastic modulus in megapascals	Poisson's ratio
Cortical bone	13,700	0.3
Trabecular bone	1370	0.3
Titanium	110,000	0.35
Resin cement	18,600	0.28
Zirconia	210,000	0.26

canine maxillary teeth at an angle of 45° in the palatolabial direction and a force of 50 N on each tooth.

c) Mesh size of the model varied from 0.1 mm to 1 mm. Implant, abutment and screws, and bone around implant were meshed with a mesh size of 0.1 mm. The mesh size gradually increased as it moved away from the implant, reaching 1 mm in the superior region of the bone.

Results

In this study, the Von Mises stress values evaluated were located in the implant neck and abutments after loading, and the maximum and minimum principal stress values investigated were in cortical and trabecular bone. Five different models were investigated by placing hexagonal and non-hexagonal titanium base abutments in different combinations on the implants placed in edentulous sites of the maxillary right canine, maxillary right central incisor, and maxillary left canine.

Von Mises stress values (Table 2) and stress distributions, demonstrated in various colors in Fig. 3, located in the implant neck region as a result of loading were analyzed. The overall stress values were higher when using the hexagonal abutments. The highest von mises value (64.71 MPa) was seen in the maxillary left canine on model 5 when using a hexagonal abutment. The lowest von mises value (56.69 MPa) was seen on the maxillary right canine on model 4 when using a non-hexagonal abutment.

Table 2 Von Mises Stress values (Mpa = megapascal) for each implant, abutment, cortical and trabecular bone.

Implant no	IVM (implant)			AVM(abutment)		
	13	11	23	13	11	23
Model 1	64.30	66.96	94.41	73.50	84.56	122.65
Model 2	64.63	71.46	94.70	73.78	84.50	123.05
Model 3	56.96	71.16	94.70	76.25	89.18	123.07
Model 4	56.69	70.24	94.44	75.97	93.96	122.67
Model 5	64.71	72.01	98.96	73.66	90.18	114.21
Implant no	Cmax			Cmin		
	13	**11**	**23**	**13**	**11**	**23**
Model 1	29.50	3.66	29.18	−4.29	−11.38	−10.68
Model 2	29.53	3.45	29.25	−4.35	−10.50	−10.73
Model 3	30.82	3.42	29.22	−4.72	−10.45	−10.73
Model 4	30.73	3.70	29.14	−4.70	−11.33	−10.69
Model 5	29.67	3.45	28.31	−4.30	−10.55	−10.24
Implant no	Tmax			Tmin		
	13	**11**	**23**	**13**	**11**	**23**
Model 1	1.29	1.95	1.76	−0.47	−0.64	−0.62
Model 2	1.32	1.87	1.68	−0.48	−0.78	−0.51
Model 3	1.34	1.87	1.76	−0.48	−0.65	−0.62
Model 4	1.34	1.90	1.76	−0.47	−0.62	−0.62
Model 5	1.29	1.89	1.84	−0.48	−0.66	−0.62

Abbreviations:
IVM; implant von mises, AVM; abutment von mises.
CMax; cortical bone maximum principle stress, CMin; cortical bone minimum principle stress.
Tmax; trabecular bone maximum principle stress, Tmax; trabecular bone minimum principle stress.

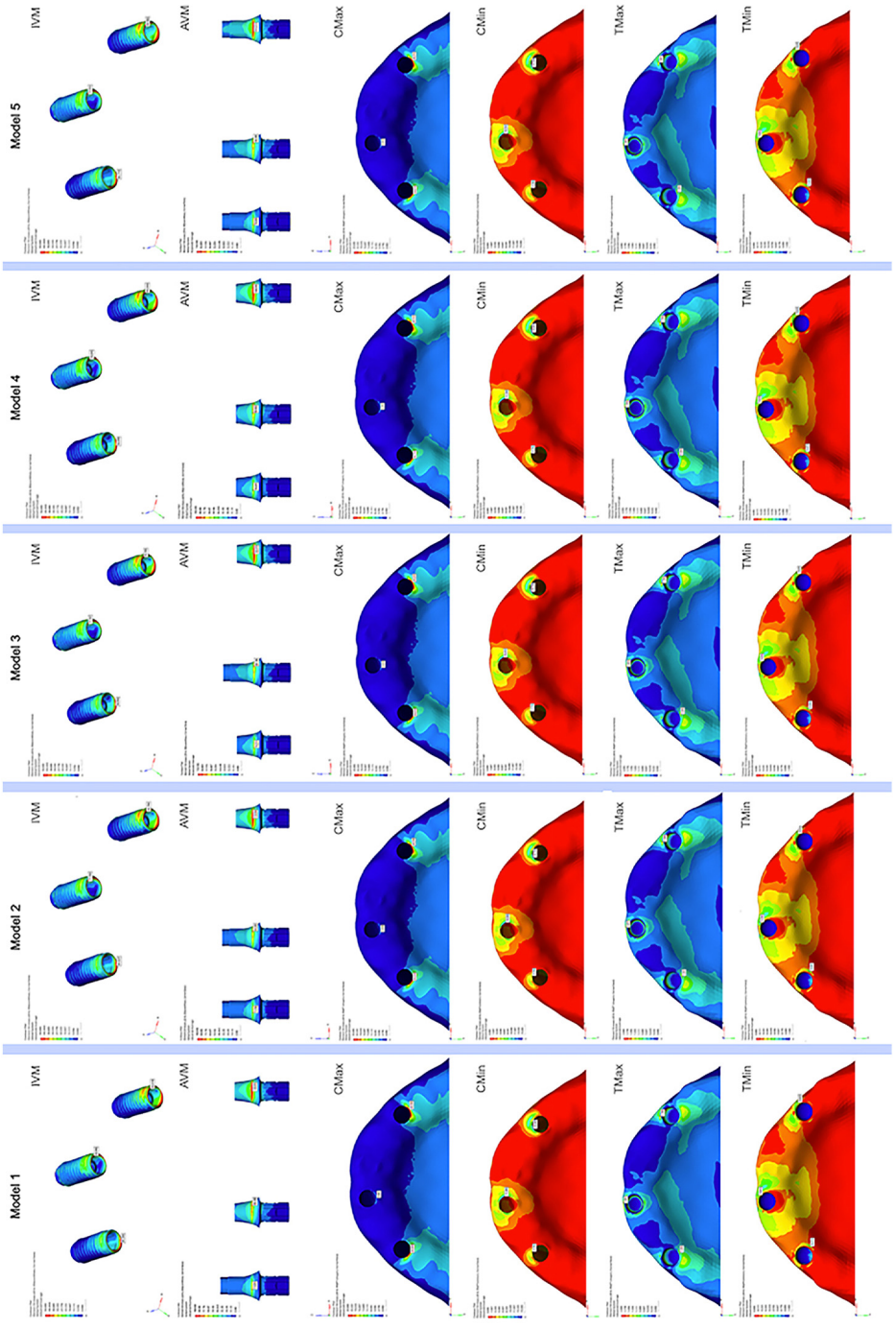

Fig. 3 Von Mises Stress distribution on each implant, abutment, cortical and trabecular bone due to loading. *Abbreviations:* IVM; implant von mises, AVM; abutment von mises. CMax; cortical bone maximum principle stress, CMin; cortical bone minimum principle stress. Tmax; trabecular bone maximum principle stress, Tmax; trabecular bone minimum principle stress.

This study also investigated the Von Mises stress values located on the abutment as a result of loading and the stress distributions in Table 2. The highest von mises value was (123.07 MPa) measured on the implant was shown on the maxillary left canine on model 3 when using the non-hexagonal abutment. The lowest stress value (73.50 MPa) was seen on the implant with a hexagonal abutment in place of the maxillary right canine.

Overall, when investigating the stress distribution on the implant neck and abutments, the results indicated the implant located in the edentulous site of the left maxillary canine had the highest stress values. The lowest overall stress distribution was displayed on the implant in site of the right maxillary canine (Table 2). When comparing the stress distribution between the five different models, the model 5 with all hexagonal abutments displayed the greatest amount of stress distribution while model 4 with all non-hexagonal abutments had the lowest stress distributed on the implant.

Additionally, the impact of the different abutments on the trabecular and cortical bone was studied. The maximum principal stress values (Table 2) and the distribution of maximum principal stresses in cortical bone due to loading were analyzed. Model 3 displayed the greatest stress (30.82 MPa) on the right maxillary canine while the lowest stress value (3.426 MPa) was observed on the maxillary right central incisor. The minimum principal stress values occurring in the cortical bone as a result of loading are shown in Table 1 and the stress distributions are shown in Fig. 3. The lowest value (−11.385 MPa) was reported for the maxillary right central incisor on model 1 when using a non-hexagonal abutment. The highest value (−4.350 MPa) was reported in model 3 when using a non-hexagonal abutment in implant site of the maxillary right canine.

Maximum principal stress values (Table 2) and the stress distribution (Fig. 3) in trabecular bone were studied as well as the minimum principal stress values (Table 2) and its stress distribution as a result of loading. The greatest stress (1.956 MPa) was reported on the maxillary right central incisor of model 4 while the maxillary right central incisor on model 1 reported the lowest stress value (1.293 MPa). The minimum principal stress value had the highest value (−0.473 MPa) for model 4 at the site of the maxillary right canine and the lowest value (−0.787 MPa) was obtained for model 2 in the area of the maxillary right central incisor.

Discussion

This study aimed to assess the effect of different abutment combinations on the forces present on the implant, implant abutment, and bone. These different implant components and designs play an important role in the stress distribution on the implants and the surrounding bone.

When evaluating the overall stress distribution placed on the implant neck, the hexagonal abutments reported higher overall stress values in comparison to the non-hexagonal abutments. The maxillary left canine on model 5 presented with the highest von mises value (98.96 MPa) when using a hexagonal abutment while the lowest value (56.69 MPa) was seen on the maxillary right canine when utilizing a non-hexagonal abutment on model 4. Overall, when using all hexagonal abutments as seen in model 5, the overall stress values were the highest compared to the other combinations. While using all non-hexagonal abutments as depicted on model 4, the overall stress values among the three implants was the lowest when compared to the other models. A similar analysis was found in a previous study by Wu et al.,[18] in which the impact of the loading position and implant design on a four-implant supported fixed prothesis was evaluated. Three types of loads were investigated including central incisor (position 1), molar region (position 2), and denture cantilever (position 3). The stresses in the cortical bone were high in the crestal region around the distal implant, especially for loading conditions 2 and 3. In this in vitro study, loading position 3 reported 36—42% and 57—62% higher peak bone stresses when compared to loading positions 2 and 1, respectively. Additionally, the highest stresses in the implant were measured near the connection between the fixture and the abutment.

Additionally, the different abutments were studied to determine the effect on the trabecular and cortical bone in this present study. The maximum principal stress values (Table 1) and the distribution of maximum principal stresses in cortical bone and trabecular bone due to loading were analyzed. Model 3 displayed the greatest cortical bone stress (30.82 MPa) while using a non-hexagonal abutment on the right maxillary canine whereas the lowest cortical bone stress (3.426 MPa) while using a hexagonal abutment was observed on the maxillary right central incisor. The highest trabecular bone stress value (1.95 MPa) and the lowest stress value (−0.78 MPa) was reported on the implant located in the site of maxillary central incisor in models 1 and 2, respectively. Similar studies are found in literature focusing on comparable topics such as a previous study by Oliveira et al.,[19] In their study, they assessed how the different implant designs [Essential Cone (implant A), Vega (implant B), and Vega+ (implant C)] impact the stress distribution (von mises) on the implants and its surrounding bone, including three types of cortical bone and two types of medullar bone. Their results indicated that stress distribution was highest for implant A and lowest for implant C for all different types of bone. When analyzing the stress distribution in bone, the maximum values of von Mises stress are localized at the cortical bone surrounding the dental implant. Higher results at the cortical bone were reported when the medullar bone density was lower (150 HU) and while the cortical bone was thinner (0.5 mm and 1.0 mm at 170.31 and 231.97 MPa, respectively).

A previous study by Nie et al.,[20] completed a similar assessment as the present study by evaluating implant abutment design (internal bone level, tissue level, and a two piece design) and microgap formation on the stress distribution on both the implant and the surrounding bone, including different bone qualities (type II, III, and IV). This previous study reported that the two-piece design with type II bone displayed minimum stress (356.55 MPa) in the implants, whereas the maximum stress occurred in the bone level design with type IV bone (578.29 MPa). The tissue level implants reported smaller stresses than those in the bone level implants when investigating all three loading conditions. When assessing the stresses in the abutments the lowest stresses were observed in the tissue level with

type IV bone group (115.02 MPa), while the highest were observed in the two-piece with type IV bone group (607.63 MPa). Similar to the analysis by Nie et al.,[20] this present study also investigated the von Mises stress values found in different abutments as a result of loading and stress distributions. The implant with a non-hexagonal abutment located in the site of maxillary left canine on model 3 reported the highest von mises value (123.07 MPa) while the lowest stress value (73.50 MPa) was seen on the implant with a hexagonal abutment in place of the maxillary right canine in model 1.

The findings of this study indicated that both the type of abutment (hexagonal and non-hexagonal) and the different abutment combinations had a comparable impact on how stress was distributed within the implant system. When assessing stress levels, there were similar values observed when comparing the cortical bone to the trabecular bone. Ultimately, hexagonal abutments exhibited the highest stress concentration in the region around the implant neck. However, when using the hexagon abutments, lower stress values was seen in the abutment at the implant-abutment junction area.

Certain limitations should be considered for the present study. First of all, the force applied in the simulation was unidirectional but forces from other regions and directions may create different outcomes intraorally. Secondly, five different elastic modulus values were used in this study but they may not be exactly the same for all people/materials. Thirdly, external factors such as saliva, temperature variation, or the presence of different antagonist materials were not considered. Lastly, the materials (implants, abutments, screws, etc) were considered to be ideals, without defects on their structure as well as with ideal contacting surfaces, which may not be the case for every restoration. Further clinical studies should search these factors to better understand their mechanical effects on the implant-supported fixed dental prosthesis.

Declaration of competing interest

The authors have no conflicts of interest relevant to this article.

Acknowledgments

This work was not supported by any organizations.

References

1. Turkyilmaz I, Unsal GS. Full-mouth rehabilitation of an elderly patient with Sjogren's syndrome by using implant-supported fixed dental prostheses including CAD/CAM frameworks. *J Dent Sci* 2019;14:428—9.
2. Arikan H, Muhtarogullari M, Uzel SM, et al. Accuracy of digital impressions for implant-supported complete-arch prosthesis when using an auxiliary geometry device. *J Dent Sci* 2023;18. 808-3.
3. Turkyilmaz I, Benli M, Schoenbaum TR. Clinical performance of 11,646 dental implants using surgical guides and two different surgical approaches: a systematic review and meta-analysis. *Int J Oral Maxillofac Implants* 2023;38(suppl):16—29.
4. Zheng Z, Ao X, Xie P, Jiang F, Chen W. The biological width around implant. *J Prosthodont Res* 2021;65:11—8.
5. Tarnow D, Hochman M, Chu S, Fletcher P. A new definition of attached gingiva around teeth and implants in healthy and diseased sites. *Int J Periodontics Restor Dent* 2021;41:43—9.
6. Naert I, Duyck J, Vandamme K. Occlusal overload and bone/-implant loss. *Clin Oral Implants Res* 2012;23(suppl):95—107.
7. Chang M, Chronopoulos V, Mattheos N. Impact of excessive occlusal load on successfully-osseointegrated dental implants: a literature review. *J Investig Clin Dent* 2013;4:142—50.
8. Turkyilmaz I, Tozum TF. Enhancing primary implant stability by undersizing implant site preparation: a human cadaver study. *J Stomatol Oral Maxillofac Surg* 2020;121:58—62.
9. Huang YC, Huang YC, Ding SJ. Primary stability of implant placement and loading related to dental implant materials and designs: a literature review. *J Dent Sci* 2023;18:1467—76.
10. Pan CY, Liu PH, Tseng YC, Chou ST, Wu CY, Chang HP. Effects of cortical bone thickness and trabecular bone density on primary stability of orthodontic mini-implants. *J Dent Sci* 2019;14: 383—8.
11. Zupancic Cepic L, Frank M, Reisinger A, Pahr D, Zechner W, Schedle A. Biomechanical finite element analysis of short-implant-supported, 3-unit, fixed CAD/CAM prostheses in the posterior mandible. *Int. J. Implant Dent.* 2022;8:8.
12. Huang LS, Huang YC, Yuan C, Ding SJ, Yan M. Biomechanical evaluation of bridge span with three implant abutment designs and two connectors for tooth-implant supported prosthesis: a finite element analysis. *J Dent Sci* 2023;18:248—63.
13. Savignano R, Soltanzadeh P, Suprono MS. Computational biomechanical analysis of engaging and nonengaging abutments for implant screw-retained fixed dental prostheses. *J Prosthodont* 2021;30:604—9.
14. Vetromilla BM, Brondani LP, Pereira-Cenci T, Bergoli CD. Influence of different implant-abutment connection designs on the mechanical and biological behavior of single-tooth implants in the maxillary esthetic zone: a systematic review. *J Prosthet Dent* 2019;121:398—403.
15. Barbosa GF, Dotto DP. Prosthetic solution for fixed full-arch maxillary prosthesis with implant divergent parallelism greater than 45°. A case report. *Stomatol* 2019;21:62—4.
16. Turkyilmaz I. Restoring severely angled implants with custom abutments and a screw-retained fixed dental prosthesis. *J Dent Sci* 2019;14:107—8.
17. Rutkunas V, Dirse J, Kules D, Simonaitis T. Misfit simulation on implant prostheses with different combinations of engaging and nonengaging titanium bases. Part 1: stereomicroscopic assessment of the active and passive fit. *J Prosthet Dent* 2023; 129:589—96.
18. Wu AY, Hsu JT, Fuh LJ, Huang HL. Biomechanical effect of implant design on four implants supporting mandibular full-arch fixed dentures: in vitro test and finite element analysis. *J Formos Med Assoc* 2020;119:1514—23.
19. Oliveira H, Brizuela Velasco A, Ríos-Santos JV, et al. Effect of different implant designs on strain and stress distribution under non-axial loading: a three-dimensional finite element analysis. *Int J Environ Res Publ Health* 2020;17:4738.
20. Nie H, Tang Y, Yang Y, Wu W, Zhou W, Liu Z. Influence of a new abutment design concept on the biomechanics of peri-implant bone, implant components, and microgap formation: a finite element analysis. *BMC Oral Health* 2023;23:277.